Study of the Reaction $\gamma\gamma \to K^+K^-$

Evan A. Variano

Department of Physics, Princeton University, Princeton, NJ 08544

Abstract

In this study we look at K^+K^- pairs that are created via two-photon interactions from electron-positron collisions with E_{CM} ∼10 GeV in CESR. The events studied have $M_{K\overline{K}}$ between 1 and 2 GeV and were detected by CLEO II. CLEO's large dataset allows us to go far beyond ARGUS's 1990 study. Specifically, our high-statistics data allows us to plot the decay angular distribution as a function of mass, with which we can identify tensor and scalar resonances. Results of this study will include measurement of the helicities of the tensor resonances a_2, f_2, and f_2'. In addition, we hope to be able to make the first measurements of $K\overline{K}$ scalar resonances in two-photon reactions and investigate the hypothesized glueball state between 1500 and 1800 MeV.

Introduction

Two-photon collisions provide a powerful way to study the quark content of resonances because the photons couple directly to the charge of the constituent quarks. The coupling strength does not only depend on the charge but also on the volume in which the quarks are created, thus the measurement of two photon couplings allows, in principle, the measurement of the size of the resonances. As a result, ground state $q\overline{q}$ resonances can be distinguished from radial excitations. In addition, glueballs (with no constituent charge) are not expected to be produced in large amounts from two-photon reactions. The absence of a signal for a known resonance in a two-photon analysis suggests a glueball nature for that resonance.

We are conducting this study of $\gamma\gamma \to K^+K^-$ in order to measure the helicities of known scalar resonances, $a_2(1320)$, $f_2(1270)$, and $f_2'(1525)$, as well as to find new resonances. We expect to observe scalar resonances, and will examine the region where $M_{K\overline{K}}$ is between 1500 and 1800 MeV, to look for evidence of a predicted scalar glueball.

The initial study of $\gamma\gamma \to K^+K^-$ was performed by ARGUS [1]. This published study looked only at the mass spectrum of tensor resonances, and was not able to investigate the helicities of these. In our study we have significantly more data, between ∼7,000 and ∼14,000 selected K^+K^- events (depending on our particle identification criteria) compared to ARGUS's ∼2,000. Because of this, we are able to plot the decay angular distribution as a function of mass, which allows us to determine the helicities of each resonance.

The decay angle used in this study is the angle at which the K^+K^- pair decays with respect to the direction of travel of the parent particle. It is written as θ^*, the asterisk denoting that the value is measured in the rest frame of the parent particle. The value θ, with no asterisk, denotes p_z/p_{total} in the lab frame for a single track, which gives the angle between the beam axis and the direction of travel of a kaon track.

An extremely important element in this analysis is the determination of the efficiency. We use Monte Carlo simulations of the reaction and the detector, from which an efficiency

plot is created. This efficiency is fitted to several models, which can then be used to account for the efficiency when describing the data.

Data

The data used is from CLEO II, data sets 4s2 through 4sG. 4s2 begins with run number 33607 and 4sG ends with run number 68027. Two-track skims are read from tape and through event selection. The event selection includes criteria similar to those commonly used in two-photon analyses [2]. We demand two good quality tracks of opposite charge, and ensure this by requiring a total charge of zero. We perform a muon veto for non-zero penetration into the iron absorber. We use standard criteria for 3-dimensional impact parameter, *i.e.*, we accept events whose tracks can be traced back to within ± 5 cm of the nominal vertex (z=0) along CLEO's beam axis and within 5 mm of the vertex radially. We require the total visible energy to be less than 6 GeV to select low-energy $\gamma\gamma$ interactions, eliminating contamination from higher-energy processes. By requiring total unmatched energy to be less than 0.5 GeV, we make sure that tracks in the drift chamber match well with activated clusters of CsI crystals (*i.e.*, we eliminate uncharged particles such as photons). We require that the total transverse momentum $p_\perp$ of the event is less than 0.2 GeV so as to select two-photon interactions in which both photons are approximately real. We identify and reject electrons by discarding tracks with $E/p > 0.85$ or $E/p < 0.02$. We require acoplanarity to be less than 0.05 radians, ensuring that both tracks are colinear in the radial projection. We require acolinearity to be greater than 0.1 radians, which selects events that are not colinear in 3 dimensions in the lab frame, eliminating background from our data set. For all selected events, we write important information into an ntuple (a multidimensional array) for analysis.

TABLE 1. Particle Identification Criteria.

criteria A	no protons, no pions, and 2 kaons
criteria B	no protons, no pions, and 1 kaon.
criteria C	no protons, no pions, and 1 kaon. Both tracks $\lvert\cos\theta\rvert < 0.8$
criteria D	no protons, no pions, and 1 kaon. Identified kaon track $\lvert\cos\theta\rvert < 0.8$

Particle identification is obtained from dE/dx, the energy loss each track undergoes while passing through the drift chamber. We compare the measured dE/dx for a track with the theoretical value for different particles. If the measured dE/dx is more than 3 standard deviations (3σ) away from the theoretical value, there is 99.7 percent probability that the track is not from that particle. If the dE/dx is within 3σ of the theoretical value for a pion, kaon, or proton, a logical flag is set in the ntuple denoting the possibility of the track (1 or 2) being this particle.

The energy loss dE/dx varies with momentum, and in the momentum range we are studying, the dE/dx curve for pions is quite close to the dE/dx curve for kaons (often within 2σ). Therefore it is quite possible for a track to have a flag set for both kaon and pion identification. We thus set criteria which look at combinations of these flags in order

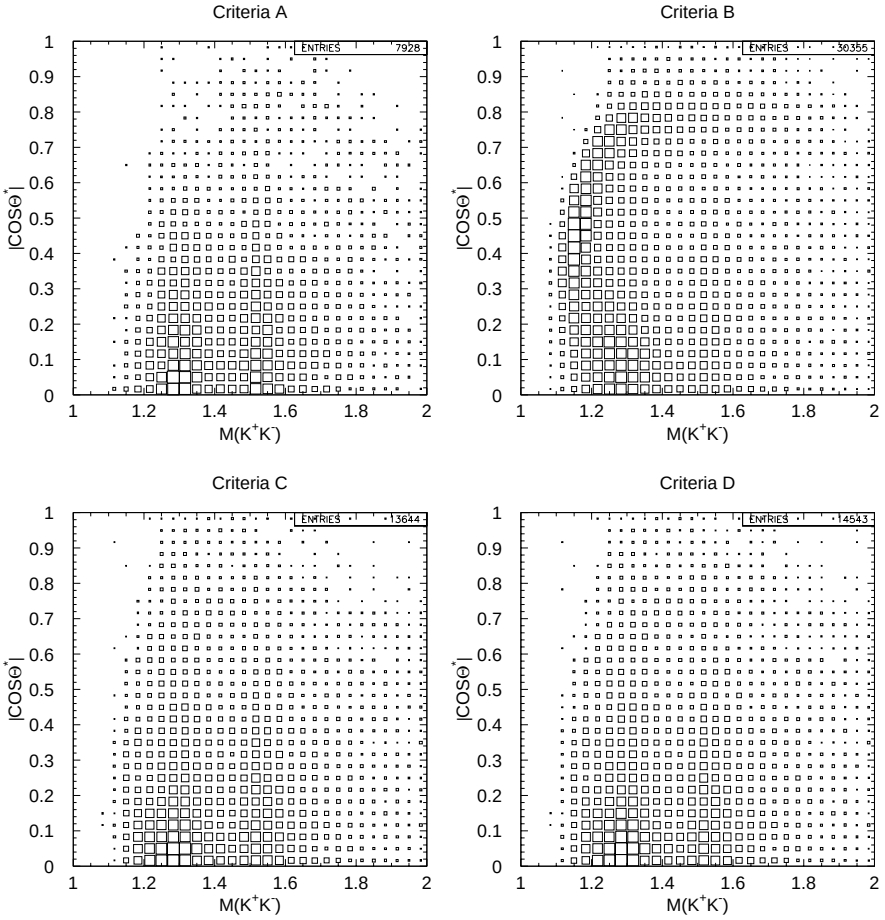

FIGURE 1. $M_{K\overline{K}}$ vs $|\cos\theta^*|$, sum over all data (not corrected for efficiency).

to select only kaon pairs. We use several sets of criteria, trying to maximize data while preserving the purity of our data set. These criteria are listed in Table 1 and a plot of $M_{K\overline{K}}$ vs $|\cos\theta^*|$ (not corrected for efficiency) for each are shown in Fig. 1.

Criteria A is the most stringent, but will reject perfectly good kaon pairs if either track has a chance at being a pion. Criteria B is based on the fact that kaons are always produced in pairs, and if we have one positively identified kaon, the other track must be a kaon as well. However, particle identification is quite poor at small decay angles in the lab frame. We see that criteria B runs the risk of accepting an event as a kaon pair based on a track which is at an unreliably small angle. Criteria C and D attempt to solve this problem; criteria C discards any event with small-angle decays as unreliable, criteria D requires that only the identified kaon have a reliable decay angle.

When comparing the data which has been evaluated with criteria A, C, and D, we see little difference in shape, but a significant difference in number of events. This suggests that all methods reliably select kaon pairs. Criteria B, however, has accepted many more events in the 1.2 GeV mass area. By looking at data which has not undergone any particle identification criteria, and is dominated by pions, we see that the large peak in the data for

Criteria B is most likely from pions which have been misidentified.

For each data set and each set of criteria, we fill the data into a 2-dimensional histogram, plotting $M_{K\overline{K}}$ vs $|(\cos\theta^*)|$. For this plot, $M_{K\overline{K}}$ is plotted directly from the ntuple, and $|(\cos\theta^*)|$ is computed via a `Fortran` routine. This reads the decay angle of each particle in the lab frame from the ntuple and uses a Lorentz transformation to compute the decay angle (equal for both particles) in the center of mass frame. This is computed with respect to the parent particle's direction of flight, which is often not exactly along the z-axis of the detector due to the initial momenta of the photons. In our analysis, the sign of $\cos\theta^*$ does not matter, and thus we take the absolute value.

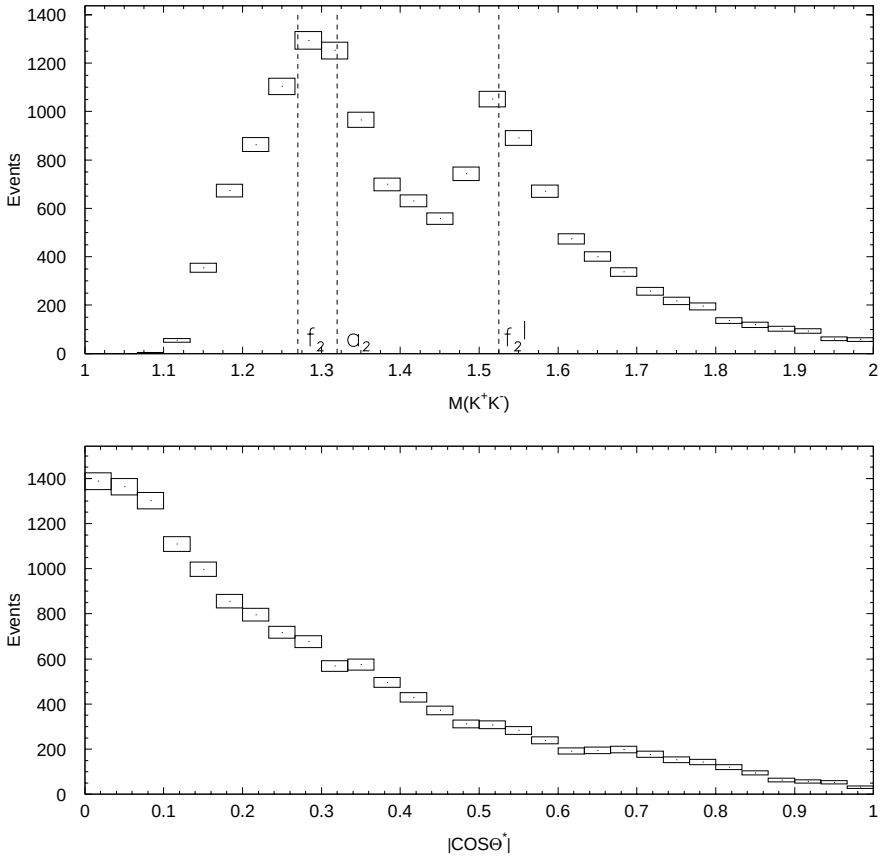

FIGURE 2. Mass spectrum and decay angle distribution, sum over all data (not corrected for efficiency). Events selected with criteria D

Shown in Fig. 2 are the projections in $M_{K\overline{K}}$ and $|(\cos\theta^*)|$ of the 2-dimensional plot $M_{K\overline{K}}$ vs $|(\cos\theta^*)|$. These plots were selected with criteria D and are not corrected for efficiency. The dotted lines in the $M_{K\overline{K}}$ plot indicate the resonances a_2, f_2, and f_2'. This plot exhibits the expected mass peaks at the resonances, including the peak resulting from a_2 and f_2 interfering constructively[1]. The shape of the $|(\cos\theta^*)|$ spectrum suggests that the reaction is dominated by tensor resonances with helicity 2, but definitive measurements of helicity cannot be made without a full partial wave analysis and correction for detector efficiency.

[1]In the reaction $\gamma\gamma \to K_s^0 K_s^0$, also being studied at Cornell, the a_2 and f_2 resonances interfere destructively.

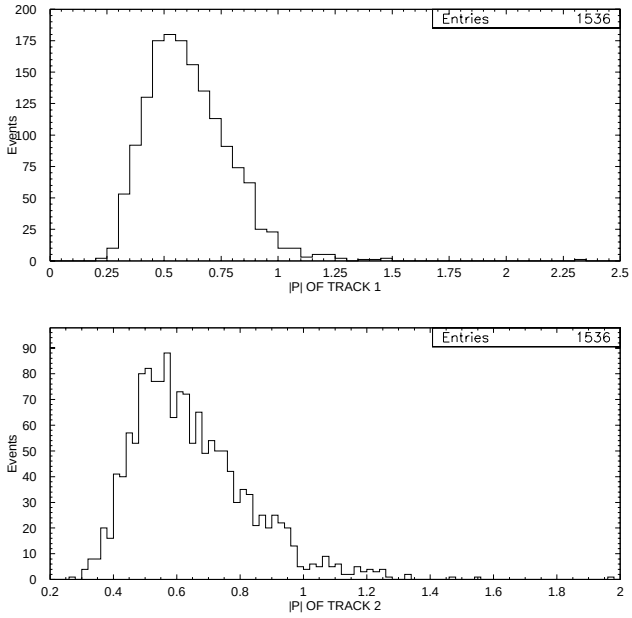

FIGURE 3. Absolute value of momentum of tracks 1 and 2 for events selected with criteria D from data set 4s2.

There was a mistake made in the computation of dE/dx for the data sets we are using, which effects tracks with $p < 300$ MeV/c. Approximately 1 percent of tracks in our data have a momentum below this value, as seen in Fig. 3.

Monte Carlo

We obtain Monte Carlo events by throwing two-photon events in `GAMGAM` [3], which is set to only produce kaon pairs. Events are thrown equally in $|\cos\theta^*|$ and are thrown in the mass range set by a control file. `GAMGAM` produces 4-vectors which are passed through the detector simulation `CLEOG` (which accounts for the detector, noise, and trigger conditions). Events are run through the same event selection as data, and ntuples are written which store all generated events (those that have not yet gone through the detector simulation) and all reconstructed events (those that have gone through the detector simulation). We began Monte Carlo by throwing 6 sets of continuum $\gamma\gamma \to K^+K^-$ events. Each was generated so as to have approximately 18,000 events. These continua were thrown across the full $M_{K\overline{K}}$ spectrum of interest, from threshold (twice the kaon mass) to 2.1 GeV. They show an strong $M_{K\overline{K}}$ dependence, having many more events in the low $M_{K\overline{K}}$ region. We improve the efficiency of the event generation by throwing in small $M_{K\overline{K}}$ intervals, rather than over the full mass range at once. Continua 7-12 were created this way, but exhibited similar $M_{K\overline{K}}$ dependence. This is because the hit and miss method employed by `GAMGAM` requires an input of maximum weighting. The weights decrease with $M_{K\overline{K}}$, and thus using a maximum weighting suitable for low masses in a high-mass region will yield a lower percentage of events. In throwing continua 13-23, we change the weighting to correspond with the $M_{K\overline{K}}$ range. At the time of completion of this paper, continua 1-6 and 13-18 have been implemented in

the efficiency analysis.

The portion of `CLEOG` which processes events across many data sets, with proper proportions, is inoperative. As a result, we processed all our events for the 4sC data set (Run numbers 63086-64026), in the on-resonance mode. 4sC was chosen after it appeared to be more resistant to `CLEOG's` tendency to crash during event processing than other single data sets which we tried. Later, it became apparent that this probably is not the case. Monte Carlo continua are shown in Table 2.

TABLE 2. Monte Carlo Continua.

continuum	mass range	random seed	events selected
c1	threshold-2.1	1	12,144
c2	threshold-2.1	2	18,000
c4	threshold-2.1	4	18,000
c5	threshold-2.1	5	13,825
c6	threshold-2.1	6	18,000
c13	threshold-1.1	1	24,000
c14	1.1-1.3	3	24,000
c15	1.3-1.5	1	24,000
c16	1.5-1.7	3	24,000
c17	1.7-1.9	1	8,968
c18	1.9-2.1	3	24,000
c19	1.0-1.2	2	30,000
c20	1.2-1.4	4	19,196
c21	1.4-1.6	2	17,725
c22	1.6-1.8	4	10,674
c23	1.8-2.0	2	20,101

Efficiency

For use in understanding the data, we plot and fit the efficiency based on our Monte Carlo events. We make a 2-dimensional efficiency histogram for $M_{K\overline{K}}$ vs $|\cos\theta^*|$ by dividing each of the 4 histograms of reconstructed events (corresponding to criteria A through D) by the histogram of generated events. We make a corresponding 2-dimensional histogram with the errors for this 2-dimensional efficiency histogram. The error function used is appropriate if we have enough data points in each histogram bin to consider the bin content to be Gaussian distributed. However, many of our bins have too few events (fewer than 5), and thus we do not want to rely on the error histogram for calculation purposes. As a result, fits for the 2-dimensional $M_{K\overline{K}}$ vs $|\cos\theta^*|$ efficiency were performed using a binned maximum likelihood method. We used 6 fit models, which are shown in Table 3.

TABLE 3. 2-Dimensional Efficiency Fit Models ($x \equiv M_{K\overline{K}}, y \equiv |\cos\theta^*|$)

model	formula	parameters
1	$[A - e^{(-B+Cy)(x-(D+Fy))}](G - Hy)(J - Kx)$	9
2	$Ax^2 + Bx + Cxy + Dy + Fy^2 + G$	6
3	$[A - e^{(-B+Cy)(x^2-(D+Fy))}](G - Hy)(J - Kx)$	9
4	$[A - e^{(-B+Cy)(x-(D+Fy))}](G - Hy)(J - K/(x - L))$	10
5	$[A - e^{(-B+Cy)(Dx^2+x-(F+Gy))}](H - Jy)(K - Lx)$	10
6	$[A - e^{(-B+Cy)(Dx^2+x-(F+Gy))}](H - Jy)(K - Lx + Mx^2)$	11

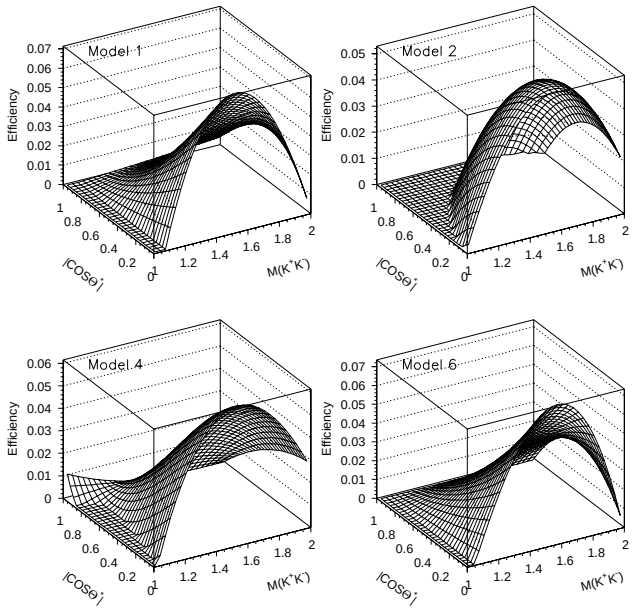

FIGURE 4. Several fit models. All events selected with criteria A.

We began fitting by examining the 2-dimensional efficiency plot and constructing fit functions that have comparable projections in $M_{K\overline{K}}$ and $|\cos\theta^*|$. Once we had a trial function, we fitted the parameters of the model and compared the result with the 2-dimensional efficiency plot. Models 1 and 2 were the first tested, and further models all developed from model 1, because it was both a better fit and more adaptable than model 2. Models 3 and 4 were attempts to improve the fit in low $M_{K\overline{K}}$ areas, where the fit is consistently low. In both cases we added a term that drops sharply with increasing $M_{K\overline{K}}$. Model 3 was the better of these new models (neither of which were exceptional). We improved it with the added term in the exponential, and then further improved it (as model 6) by changing the linear term in x to parabolic, providing more freedom for the fit, especially in the low-$M_{K\overline{K}}$ region. The values of the log likelihood show models 1 and 6 to be the best, regardless of the particle

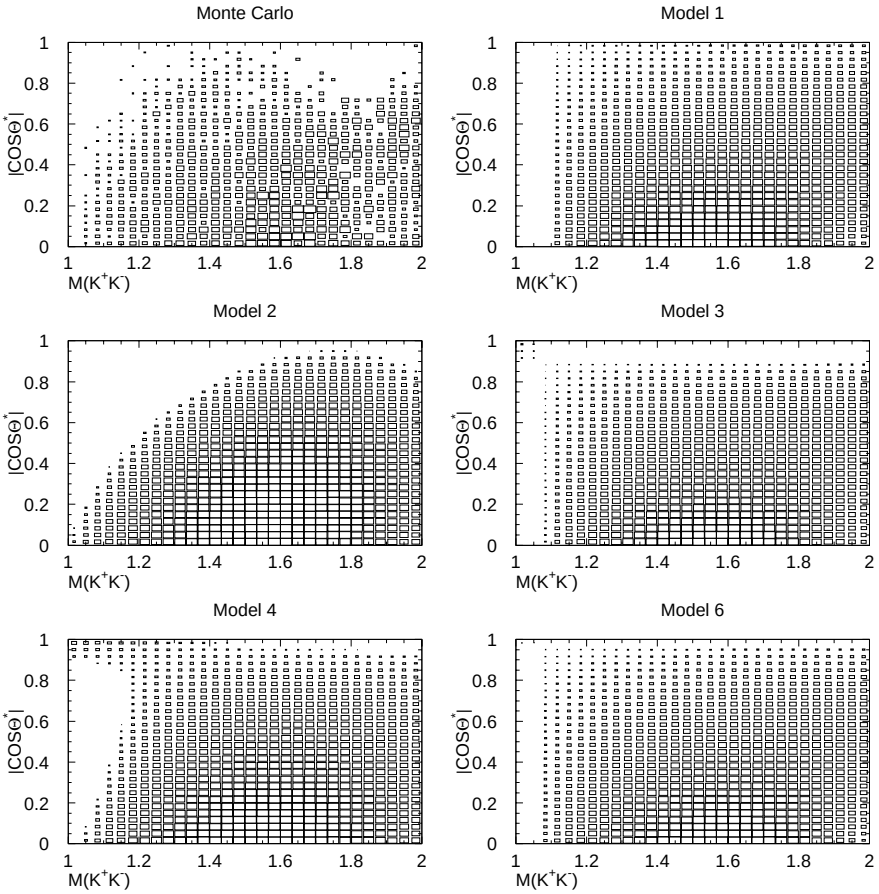

FIGURE 5. Efficiency plot from Monte Carlo events and fit models 1,2,3,4, and 6. All events selected with criteria A.

identification criteria used. Fig. 4 and Fig. 5 show plots of these models. A slice-by-slice comparison of fits and 2-dimensional efficiency supports the superiority of models 1 and 6, showing that these are the only models which demonstrate parabolic behavior in $|\cos\theta^*|$ at high $M_{K\overline{K}}$ values. Fig. 6 and Fig. 7 display such a plot, showing all slices in $|\cos\theta^*|$ for model 1 (created with 30x30 binning) and the low-$M_{K\overline{K}}$ slices in $|\cos\theta^*|$ for model 6. Models 1 and 6 are indistinguishable in higher-$M_{K\overline{K}}$ slices, and we see that model 6 is more accurate at low masses.

Summary and Outlook

We have selected $\gamma\gamma \to K^+K^-$ events from CLEO II and studied the effect of different particle identification criteria on the events selected. These criteria select events with different precision and efficiency. Regardless of the criteria used, we have significantly more events than in the previous study.

We have studied the efficiency for the process $\gamma\gamma \to K^+K^-$ as a function of $M_{K\overline{K}}$ and $|\cos\theta^*|$ and have developed models to describe this efficiency in an analytical form. We have found models which display all features of the efficiency plot created from Monte Carlo events.

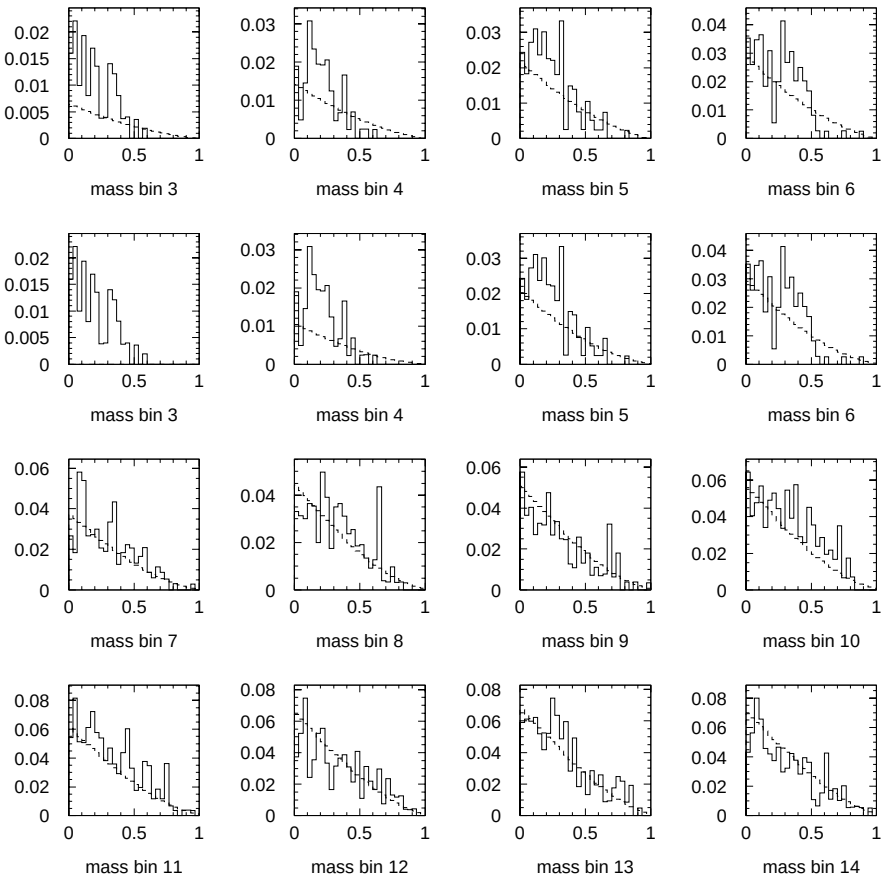

FIGURE 6. Slices in $M_{K\overline{K}}$ for models 1 and 6 (dashed lines) compared to efficiency plot from Monte Carlo (solid line). The first row represents model 6, the following rows represents model 6. All events selected with criteria A.

With these fitted efficiency functions, one is now able use the analytical form of the efficiency to begin a partial wave analysis. The data can be fit to Breit-Wigner amplitudes, taking into account the possible presence of both scalar resonances and tensor resonances with helicities 0 or 2. Before results can be considered final, one must revisit the detector simulator CLEOG, processing Monte Carlo events across all data sets in correct proportions based on the luminosities for each data set. One may wish to increase the amount of Monte Carlo so as to be able to perform a χ^2 fit on the 2-dimensional efficiency.

Acknowledgments

I am pleased to acknowledge Prof. Richard S. Galik and Dr. Sven von Dombrowski, of Cornell University. Prof. Galik proposed this Research Experience for Undergraduates project and coordinated the $\gamma\gamma$ group. Dr. Dombrowski worked closely with me during the entire project and guided my efforts. Both were extremely helpful in supervising my project and in educating me about two-photon research in specific and particle physics in general.

This work was supported by National Science Foundation grant PHY-9310764 and NSF REU grant PHY-9731882.

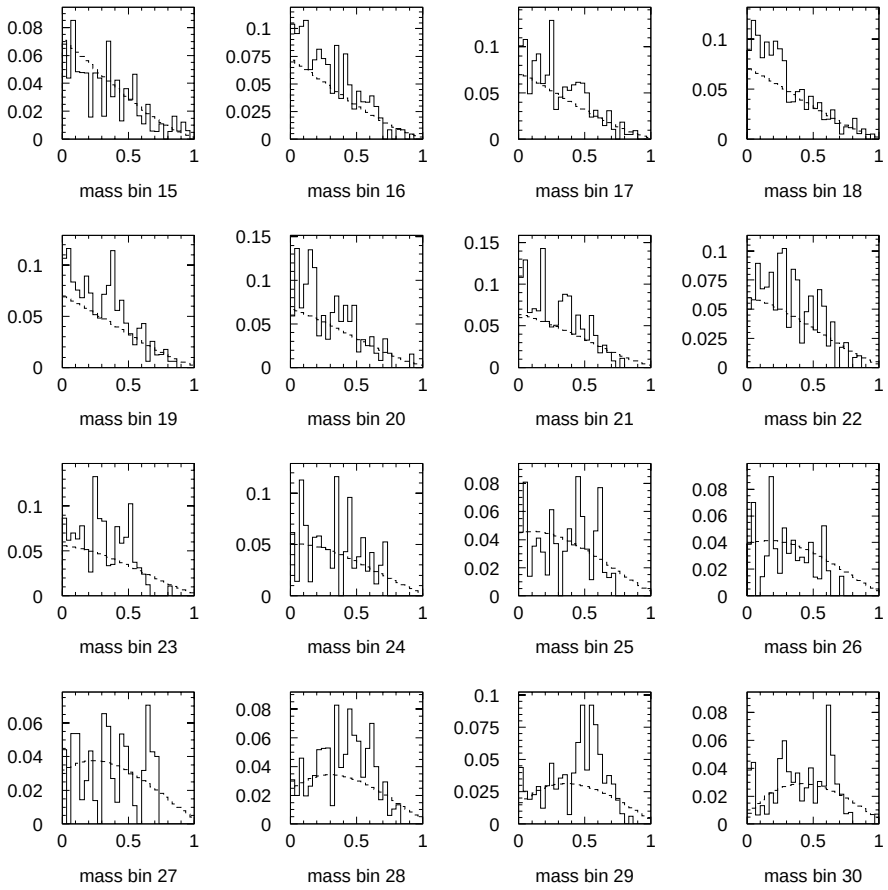

FIGURE 7. Slices in $M_{K\overline{K}}$ for model 1 (dashed line) compared to efficiency plot from Monte Carlo (solid line). All events selected with criteria A.

References

1. ARGUS Collaboration, H. Albrecht *et al.*, Z. Phys. **C 48** (1990) 183.
2. CLEO Collaboration, M.S. Alam *et al.* Further search for the two-photon production of the glueball candidate $f_J(2220)$, 1998, submitted to Phys. Rev. Lett.
3. `GAMGAM` is a Monte Carlo generator for two-photon events based on the Budnev-Ginzburg-Meledin-Serbo formalism; V.M Budnev *et al.*, Phys. Rep. **15 C** (1975) 181.